Analytical surface charge method for rotated permanent magnets : boundary element method comparison and experimental validation

Please check the document version of this publication:

• A submitted manuscript is the version of the article upon submission and before peer-review. There can be important differences between the submitted version and the official published version of record. People interested in the research are advised to contact the author for the final version of the publication, or visit the DOI to the publisher's website.
• The final author version and the galley proof are versions of the publication after peer review.
• The final published version features the final layout of the paper including the volume, issue and page numbers.
Link to publication

Download date: 16. Nov. 2023

Analytical Surface Charge Method for Rotated Permanent Magnets: Boundary Element Method Comparison and Experimental Validation

J. R. M. van Dam[1], J. J. H. Paulides[1], E. A. Lomonova[1], and M. Dhaens[2]

[1]Department of Electrical Engineering, Eindhoven University of Technology, Eindhoven 5612 AP, The Netherlands

[2]Advanced Chassis Research, Tenneco Automotive Europe BVBA, B 3800 Sint-Truiden, Belgium

This paper is concerned with the analytical calculation of the interaction force between two permanent magnets (PMs) under relative rotation by means of the surface charge method, taking into account the non-unity relative permeability of the PMs. This model combines high accuracy and a short calculation time. As the considered PM configuration is a free-space, unbounded problem, the results from the surface charge method are compared to its numerical counterpart, the Boundary Element Method (BEM). The analytical expressions were validated by means of the measurement results obtained from a 3-D printed test setup.

Index Terms—**Analytical models, electromagnetic fields, electromagnetic forces, permanent magnets.**

I. INTRODUCTION

THE increasing interest in wireless sensors and wearable electronics has encouraged the research into renewable battery-replacement technologies, as to reduce the maintenance and resource cost inseparably related to batteries. An attractive alternative is to harvest energy from natural vibration sources as they are widely available, and potentially contain a high power density. The conversion of the kinetic energy in vibrations into electrical energy has been achieved using many different types of transducers, such as mechanical [1], magnetoelectric [2], electrostatic [3], electromagnetic [4], or piezoelectric [5]–[7].

In piezoelectric cantilever beam energy harvesters [6], [7], the beam fundamental resonance frequency is usually matched with the system excitation frequency, as to yield the largest harvested energy. However, to allow for a range of excitation frequencies, the interaction forces between permanent magnets (PMs) are applied to tune the beam resonance frequency. In [7], the PM interaction forces result from an approximation function. The optimization of the energy harvesting capabilities requires an improved accuracy with respect to the determined interaction forces. Hence, a PM modeling method which provides a 3-D magnetic field solution, works well in free-space unbounded problems, handles relative rotations between PMs, and does not require periodicity of the considered magnetic structure should be considered. Moreover, to allow for fast optimization and geometry selection, an analytical model is preferred over numerical alternatives. Both the surface charge method [8]–[13] and the Boundary Element Method (BEM) [14] satisfy the above conditions.

This paper provides an improved calculation of the interaction force between two permanent magnets under relative rotation with respect to existing cantilever beam vibration energy harvesters. The analytical surface charge method and the BEM simulation results are compared to the results from the Finite Element Method (FEM). Additionally, an experimental setup is designed to validate the simulation results.

II. CONSIDERED GEOMETRY

An implementation of the considered energy harvesting cantilever beam is shown in Fig. 1. Environmental vibrations are transferred to the beam structure, where minor vibrations of the tip mass are amplified by the forces between the PMs. The beam oscillates at its resonance frequency, f_r, which is partially determined by the height and length of the beam, Δc and l, respectively, and the distance between the PMs, Δt and Δb. Energy is generated by the deformation of the piezoelectric elements in the beam. This is illustrated on an energy harvesting cantilever beam in Fig. 1, where the energy harvester consists of a non-magnetic beam to which piezoelectric elements, PMs, and a non-magnetic free end tip mass are attached. A simplified representation of the cantilever beam PMs is shown in Fig. 2, where only two PMs are considered. The PM dimensions are summarized in Table I.

III. SURFACE CHARGE METHOD FOR ROTATED PMS

Simplified two-dimensional analytical models to obtain the interaction force between magnets in radial bearings and couplings were initially proposed using superposition of the interaction force [15]–[19]. Using the magnetic imaging technique [20], a soft-magnetic slotless back-iron was incorporated in the models of the PM coupling [18]. Investigation into 3-D solutions performed in [21], [22] resulted in semi-analytical equations requiring a numerical integration of the logarithmic terms. The current sheet model used in [21], [23] employed the Lorentz force calculation for a simple topology.

The surface charge method has been a research topic as of 1984, when Akoun and Yonnet expressed analytically the magnetic field and the interaction force between two axially displaced PMs with parallel magnetization [8]. Several researchers have contributed to the model advancement, for instance by developing equations for interactions between perpendicularly magnetized PMs for multi-axial displacements [11]. More recently, a comprehensive overview of the surface charge method was composed [13], in which the force equations for rotated permanent magnets were stated, based on [9].

A short derivation of the surface charge method, resulting in expressions for the interaction force between relatively rotated

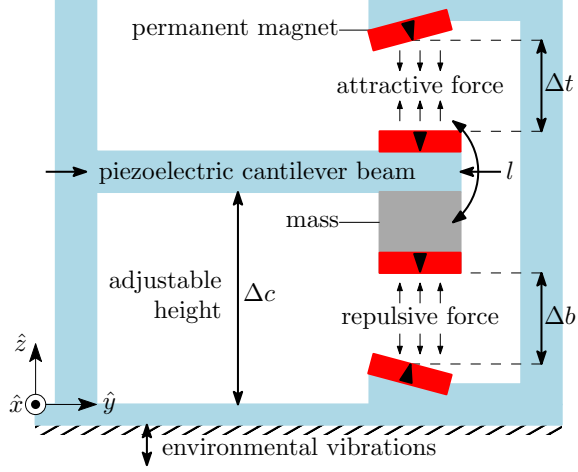| $2a_1$	17 mm	$2a_2$	17 mm	α	0 mm
$2b_1$	11.5 mm	$2b_2$	11.5 mm	β	$60\,(\cos\theta - 1)$ mm
$2c_1$	3.5 mm	$2c_2$	3.5 mm	γ	$60\sin\theta$ mm
B_r	1.18 T	μ_r	1.02		

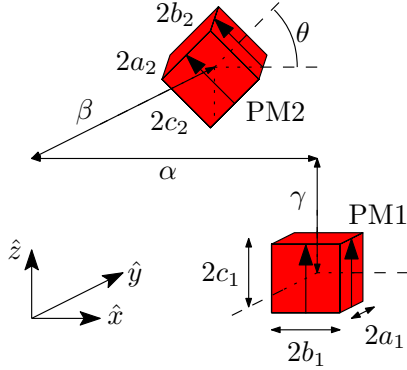Fig. 1. Energy harvesting piezoelectric cantilever beam.

Fig. 2. Two permanent magnets under relative rotation.

permanent magnets, will be presented now [10]. Starting with the magnetostatic Maxwell equations for current-free regions,

$$\nabla \times \vec{H} = 0, \qquad \nabla \cdot \vec{B} = 0,$$

the magnetic scalar potential, φ_m, is introduced by means of the vector identity $\nabla \times (\nabla \varphi_m) = 0$,

$$\vec{H} = -\nabla \varphi_m. \quad (1)$$

To relate the magnetic scalar potential to the permanent magnet magnetization vector, $\vec{M}$, substitute the constitutive relation $\vec{B} = \mu_0 \left(\vec{H} + \vec{M} \right)$ and (1) into $\nabla \cdot \vec{B} = 0$ to obtain

$$\nabla^2 \varphi_m = \nabla \cdot \vec{M}.$$

If $\vec{M}$ only exists inside a volume $\mathcal{V}$, bounded by $\mathcal{S}$, then the solution to this equation is represented by means of the free-space Green's function as

$$\varphi_m (\vec{x}) = -\frac{1}{4\pi} \int_{\mathcal{V}} \frac{\nabla' \cdot \vec{M}(\vec{x}')}{|\vec{x} - \vec{x}'|} \mathrm{d}v' + \frac{1}{4\pi} \oint_{\mathcal{S}} \frac{\vec{M}(\vec{x}') \cdot \hat{n}}{|\vec{x} - \vec{x}'|} \mathrm{d}s',$$

in which the volume charge density, $\rho_m = -\nabla \cdot \vec{M}\,(\mathrm{A/m^2})$, and the surface charge density, $\sigma_m = \vec{M} \cdot \hat{n}\,(\mathrm{A/m})$. The magnetic flux density for a uniformly magnetized permanent magnet, i.e. where $\rho_m = -\nabla \cdot \vec{M} = 0$, is calculated with

$$\vec{B}(\vec{x}) = \frac{\mu_0}{4\pi} \oint_{\mathcal{S}} \frac{\sigma_m(\vec{x}')\,(\vec{x} - \vec{x}')}{|\vec{x} - \vec{x}'|^3} \mathrm{d}s'.$$

Usually, the relative magnetic permeability, μ_r, is assumed unity in the charge method. This introduces a deviation between the analytical results, and the results from FE simulations. The correct value for μ_r is taken into account by adjusting the remanent magnetization, B_r, using [24]

$$\sigma = \frac{B_r/\mu_0}{\mu_r \left(\frac{3}{2} - \frac{\mu_r}{2} \right)}, \quad \text{and} \quad B_r = \sigma \mu_0.$$

Consider the magnets PM1 and PM2 in Fig. 2 of dimensions $[a_1, b_1, c_1]^T$ and $[a_2, b_2, c_2]^T$, respectively. Their centers are displaced by $[\alpha, \beta, \gamma]^T$, and PM2 is rotated with respect to the x-axis by an angle θ. As α is zero, and only a rotation around the x-axis is considered, F_x is zero. If θ is an integer multiple of π rad, the magnetization directions of the PMs are (anti-)parallel and F_z is calculated according to [8], [11], [13]

$$F_z|_{\theta=k\pi} = \frac{B_{r1} B_{r2} \cos(\theta)}{4\pi\mu_0}$$
$$\sum_{i,j,k,l,m,m=0}^{1} [-1]^{i+j+k+l+m+n} f_{3z}(x', y', z'), \quad (2)$$

where

$$x' = \alpha + (1-i)\,a_1 - (1-j)\,a_2,$$
$$y' = \beta + (1-k)\,b_1 - (1-l)\,b_2 + \frac{1}{2} c_2 \sin(\theta),$$
$$z' = \gamma + (1-m)\,c_1 - (1-n-\cos(\theta))\,c_2 - \frac{1}{2} b_2 \sin(\theta),$$

and, using $r = \sqrt{u^2 + v^2 + w^2}$,

$$f_{3z}(u, v, w) = uv \arctan\left(\frac{uv}{wr} \right) - wr$$
$$- \frac{1}{2} uw \ln\left(\frac{r-u}{r+u} \right) - \frac{1}{2} vw \ln\left(\frac{r-v}{r+v} \right). \quad (3)$$

The limit cases for these expressions have been derived in [25]. Complementary, for $\theta \neq k\pi$, F_z follows from [9], [13]

$$F_z = -\frac{B_{r1} B_{r2}}{4\pi\mu_0} \sum_{i,j,k,l,m,m=0}^{1} [-1]^{i+j+k+l+m+n}$$
$$\left(\frac{f_3(U, V, W, \theta, b_1 k, 0, b_2 l, 0)}{\tan\theta} \right.$$
$$\left. + \frac{f_3(UU, VV, WW, -\theta, b_1 k, 0, b_2 l, 0)}{\sin\theta} \right), \quad (4)$$

where

$$U = \alpha - (i-1)\,a_1 + (j-1)\,a_2,$$
$$V = \beta + b_1 - b_2 \cos\theta + (1-n)\,c_2 \sin\theta,$$
$$W = \gamma - (m-1)\,c_1 + (n-1)\,c_2 \cos\theta - b_2 \sin\theta,$$
$$UU = -\alpha - (i+1)\,a_1 + (j+1)\,a_2,$$
$$VV = -V \cos\theta - W \sin\theta,$$
$$WW = V \sin\theta - W \cos\theta,$$

and

$$f_3\left(u,v,w,\theta,b,c,y,z\right) = uf_5\left[\ln\left(f_4 - u\right) - 1\right] +$$
$$uf_6\arctan\left(\frac{uf_4 - f_6^2 - u^2}{f_5f_6}\right) + \frac{1}{2}\pi u\operatorname{sgn} f_5\left|f_6\right| +$$
$$\frac{1}{2}f_4f_5 + \frac{1}{2}\left(f_6^2 - u^2\right)\ln\left(f_4 + f_5\right), \quad (5)$$

in which

$$f_4 = \sqrt{u^2 + f_5^2 + f_6^2},$$
$$f_5 = y + (v - b)\cos\theta + (w - c)\sin\theta,$$
$$f_6 = z - (v - b)\sin\theta + (w - c)\cos\theta.$$

For both considered cases, the y-component of the force, F_y, is calculated according to

$$F_y = \frac{B_{r1}B_{r2}}{4\pi\mu_0}\sum_{i,j,k,l,m,m=0}^{1}[-1]^{i+j+k+l+m+n}$$
$$f_3\left(U, \beta + b_1 - b_2\cos\theta + c_2\sin\theta,\right.$$
$$\gamma + (1 - m)c_1 - b_2\sin\theta + c_2\left(\cos\theta - 1 + n\right),$$
$$\left.\theta, b_1k, c_1m, b_2l, c_2n\right). \quad (6)$$

IV. SIMULATION SETUP

Contrary to the analytical surface charge method, a numerical approach to model the permanent magnet configuration in Fig. 2 is the Boundary Element Method (BEM). The BEM is well-suited for the problem, as the considered configuration is a free-space, unbounded problem, in which the material properties are assumed linear and homogeneous. In the following, the results from the analytical surface charge method and the BEM will be compared, both to each other, as well as to FE simulation and experimental results. The applied BEM is the software package Faraday 3-D Eddy Current Solver Version 8.0, 2009 by Integrated Engineering Software. In the simulation, 972 2-D quadrilateral elements have been taken into account. The solving process of a single step takes less than a second. The applied electromagnetic 3-D FEM is Flux Version 12 Service Pack 2, 2015 by Cedrat. In the simulation, 3,621,184 volume elements have been taken into account. The solving process takes approximately 24 hours.

V. COMPARISON AND VALIDATION

The measurement results that were obtained on the 3-D printed test setup shown in Fig. 3 are used to validate the results from the charge method. The PMs were in a repulsive configuration, hence, PM1 was pushed to the load cell, whereas PM2 retained its position because of the slotted construction. A six degree-of-freedom (6-DoF) load cell was used, whose output was logged by means of a dSPACE module and a logging computer. Multiple runs were performed, and the filtered average results are displayed in Fig. 4 together with the simulation results.

Very close agreement between the charge method and the BEM is found, as the results deviate on average 0.63 %, as shown in Fig. 5. This deviation is attributed to numerical inaccuracies in the assignment of the PM dimensions. The
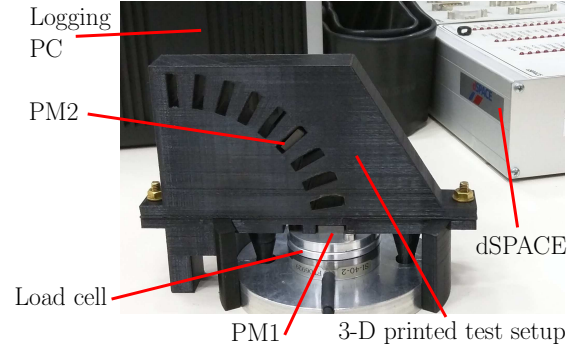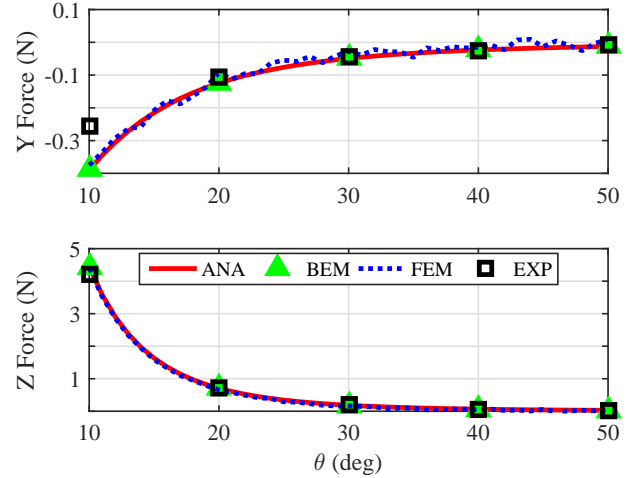

Fig. 3. The experimental setup.

Fig. 4. Comparison of the simulation and measurement results, where ANA is the analytical surface charge method, BEM is the Boundary Element Method, FEM is the Finite Element Method, and EXP are the experimental results.

results from the FEM are less accurate, which is attributed to numerical noise resulting from an insufficiently dense mesh. Such dense mesh is required, as a free-space, unbounded problem is considered, which is less suitable for the FEM as compared to the charge method and the BEM.

The measurement results confirm the simulated force development in both the y- and z-direction. However, for the smallest θ-value, the measurement results deviate, and especially the y-component deviates largely, as shown in Fig. 5. This is attributed to inaccuracies in the test setup, which are composed of deviations in the remanent magnetization and magnetization angle of the PMs, 3-D printer manufacturing tolerances, and deviations in the alignment of the test setup with respect to the xy-plane of the load cell.

VI. DISCUSSION

A close agreement between the results from the surface charge method and the BEM was found, despite the distinct differences between the methods. The BEM employs a densely populated, non-symmetric system matrix which elevates memory usage and could, potentially, increase computer times to the level of the FEM. Additionally, material properties are assumed linear and homogeneous, which renders the BEM
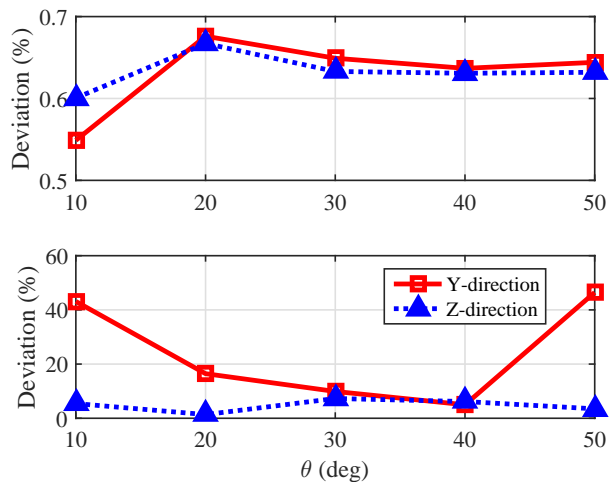
Fig. 5. Percentage deviation between the analytical surface charge method and the (top) BEM, and the (bottom) experimental results.

unsuitable for configurations involving soft-magnetic material. A major asset of the BEM surfaces when considering free-space, unbounded problems, as it only requires field source boundaries to be discretized, resulting in faster solutions than the FEM. Contrary to the BEM, the surface charge method is analytically formulated, resulting in faster solutions. As a result of recent developments, the applicability of the surface charge method has improved by (semi-)analytically including the relative permeability of soft-magnetic materials [26].

For now, the applicability of the surface charge method is limited to rotations around the x-axis, in combination with a translation with respect to the y- and z-axes. Therefore, the method does not serve FEM-replacement yet [13]. Model extensions include the forces between cylindrical PMs with single-axis rotation. Subsequently, the forces and torques between pairs of cuboidal and pairs of cylindrical PMs with arbitrary rotation should be considered. Then, expressions for the forces and torques between pairs of spherical, triangular, and differently-shaped permanent magnets should be developed.

VII. CONCLUSION

In this paper, the analytical surface charge method is applied to two relatively rotated permanent magnets (PMs). The calculated interaction force is compared to results from the Boundary Element Method (BEM), and validated against experimental results. Although the surface charge method already shows superior applicability and computational time, compared to the BEM, great promise lies in the extension of the method to allow for multi-axial rotations to provide a 6-DoF permanent magnet interaction model, which can serve as a fast, analytical replacement to the finite element method.

REFERENCES

[1] Z. Li, L. Zuo, J. Kuang, and G. Luhrs, "Energy-harvesting shock absorber with a mechanical motion rectifier," *Smart Mater. Struct.*, vol. 22, no. 2, p. 025008, 2013.

[2] J. Yang, Y. Wen, P. Li, X. Dai, and M. Li, "A Broadband Vibration Energy Harvester Using Magnetoelectric Transducer," in *IEEE Sensors*, Nov. 2010, pp. 1905–1909.

[3] A. Fowler, S. Moheimani, and S. Behrens, "An Omnidirectional MEMS Ultrasonic Energy Harvester for Implanted Devices," *J. Microelectromech. S.*, vol. 23, no. 6, pp. 1454–1462, Dec. 2014.

[4] Q. Zhang and E. S. Kim, "Vibration Energy Harvesting Based on Magnet and Coil Arrays for Watt-Level Handheld Power Source," *Proc. IEEE*, vol. 102, no. 11, pp. 1747–1761, Nov. 2014.

[5] J. Jung, P. Kim, J.-I. Lee, and J. Seok, "Nonlinear dynamic and energetic characteristics of piezoelectric energy harvester with two rotatable external magnets," *Int. J. Mech. Sci.*, vol. 92, pp. 206–222, 2015.

[6] S. R. Anton and H. A. Sodano, "A review of power harvesting using piezoelectric materials (2003-2006)," *Smart Mater. Struct.*, vol. 16, no. 3, pp. R1–R21, 2007.

[7] V. R. Challa, M. G. Prasad, Y. Shi, and F. T. Fisher, "A vibration energy harvesting device with bidirectional resonance frequency tunability," *Smart Mater. Struct.*, vol. 17, no. 1, p. 015035, 2008.

[8] G. Akoun and J.-P. Yonnet, "3D analytical calculation of the forces exerted between two cuboidal magnets," *IEEE Trans. Magn.*, vol. 20, no. 5, pp. 1962–1964, Sep. 1984.

[9] J. F. Charpentier and G. Lemarquand, "Study of Permanent-Magnet Couplings with Progressive Magnetization Using an Analytical Formulation," *IEEE Trans. Magn.*, vol. 35, no. 5, pp. 4206–4217, Sep. 1999.

[10] E. P. Furlani, *Permanent Magnet and Electromechanical Devices: Materials, Analysis, and Applications*, ser. Academic Press Series in Electromagnetism. Academic, 2001.

[11] J. L. G. Janssen, J. J. H. Paulides, E. Lomonova, F. Bölöni, A. Tounzi, and F. Piriou, "Analytical Calculation of Interaction Force Between Orthogonally Magnetized Permanent Magnets," *Sensor Letters*, vol. 7, no. 3, pp. 442–445, 2009.

[12] H. Allag, "Models and Calculation of Passive Magnetic Suspension – 2D and 3D Analytical Calculation of Interactions Between Permanent Magnets," Ph.D. dissertation, Université de Grenoble, Jun. 2010.

[13] W. S. P. Robertson, "Modelling and design of magnetic levitation systems for vibration isolation," Ph.D. dissertation, The University of Adelaide, SA, Australia, Nov. 2013.

[14] L. Gaul, M. Kögl, and M. Wagner, *Boundary Element Methods for Engineers and Scientists – An Introductory Course with Advanced Topics*, 1st ed. Springer-Verlag Berlin Heidelberg, 2003.

[15] J.-P. Yonnet, "Passive magnetic bearings with permanent magnets," *IEEE Trans. Magn.*, vol. 14, no. 5, pp. 803–805, Sep. 1978.

[16] R. Hornreich and S. Shtrikman, "Optimal design of synchronous torque couplers," *IEEE Trans. Magn.*, vol. 14, no. 5, pp. 800–802, Sep. 1978.

[17] J.-P. Yonnet, "Permanent magnet bearings and couplings," *IEEE Trans. Magn.*, vol. 17, no. 1, pp. 1169–1173, Jan. 1981.

[18] J.-P. Yonnet, S. Hemmerlin, E. Rulliere, and G. Lemarquand, "Analytical calculation of permanent magnet couplings," *IEEE Trans. Magn.*, vol. 29, no. 6, pp. 2932–2934, Nov. 1993.

[19] J. M. D. Coey, *Rare-Earth Iron Permanent Magnets*, 1st ed., ser. Monographs on the Physics and Chemistry of Materials. Oxford, U.K.: Oxford University Press, 1996, vol. 54.

[20] B. Hague, *The principles of electromagnetism applied to electrical machines*, 1st ed. New York: Dover Publications, 1962.

[21] J. Tsui, D. Iden, K. Strnat, and A. Evers, "The effect of intrinsic magnetic properties on permanent magnet repulsion," *IEEE Trans. Magn.*, vol. 8, no. 2, pp. 188–194, Jun. 1972.

[22] W. Baran, "Analytical methods for the design calculation of permanent magnet synchronous couplings," *Acta Polytechnica Scandinavica, Applied Physics Series*, no. 138, pp. 13–19, 1983.

[23] H. S. Nagaraj, "Investigation of Magnetic Fields and Forces Arising in Open-Circuit-Type Magnetic Bearings," *Tribology Transactions*, vol. 31, no. 2, pp. 192–201, 1988.

[24] M. F. J. Kremers, J. J. H. Paulides, E. Ilhan, J. L. G. Janssen, and E. A. Lomonova, "Relative Permeability in a 3D Analytical Surface Charge Model of Permanent Magnets," *IEEE Trans. Magn*, vol. 49, no. 5, pp. 2299–2302, May 2013.

[25] J. L. G. Janssen, J. J. H. Paulides, and E. A. Lomonova, *Computer field models of electromagnetic devices - Studies in applied electromagnetics series*. Amsterdam: IOS Press, 2010, ch. Analytical Force and Stiffness Calculations for Magnetic Bearings and Vibration Isolation, pp. 502–511.

[26] D. van Casteren, J. Paulides, and E. Lomonova, "Modeling the Field Inside a Soft-Magnetic Boundary using Surface Charge Modeling," *IEEE Trans. Magn.*, vol. PP, no. 99, pp. 1–1, 2015.